

# A Numerical Approach to Diffusive Slowdown in Three-Layer Hele-Shaw Flows

Prabir Daripa<sup>1,\*</sup> and G. Paşa<sup>2</sup>

<sup>1</sup>Department of Mathematics, Texas A&M University, College Station, TX-77843

<sup>2</sup>Institute of Mathematics “Simion Stoilow” of Romanian Academy, Bucharest, RO-70700

## Abstract

Effect of species diffusion as opposed to that of molecular diffusion in suppressing hydrodynamic instabilities in three-layer immiscible flows in a Hele-Shaw cell is addressed here. The approach here is constructive which relies upon stability analysis and subsequent numerical analysis of the discrete approximation of the stability equations. Upper bound on the growth rate of instabilities is derived which is then used in establishing the diffusive slowdown of instabilities. Upper bounds obtained by this numerical approach and by the analytical approach reported in this journal are compared. The present approach provides a numerical method that can be implemented in the future for further investigation of the effects of diffusion.

Keywords: Hele-Shaw Flows, Stability, Effect of Diffusion, Upper Bound, Numerical Analysis

---

\*Author for correspondence (e-mail: prabir.daripa@math.tamu.edu)

# 1 Introduction

The subject of multi-layer (more than two-layer) multi-phase flows has received much less attention than similar two-layer flows, partly because of the level of difficulty associated with studies of such flows. Such flows are usually richer in complexity and involve many parameters and variables whose control and manipulations in innovative ways can prove to be useful technologically. To make theoretical and computational advances in this direction, mathematical formulation of such problems is the first necessary step. One such problem that has received some attention (Gorell and Homsy 1983; Daripa and Pasa 1985a), partly motivated by industrial applications (Littman 1988; Needham and Doe 1987; Shah and Schecter 1977; Sorbie 1991; Uzoigwe et. al. 1974), involves three-layer immiscible flows in Hele-Shaw cells involving two sharp interfaces initially. The physical set-up of the problem involves three-layers of fluid in a Hele-Shaw cell with least viscous fluid such as water displacing an intermediate layer of fluid having variable viscosity. This layer in turn displaces the most viscous fluid such as oil. The fluid in the intermediate layer is an aqueous phase consisting of polymer in water. Pointwise viscosity of this aqueous phase (to be called ‘poly-solution’ henceforth) in this intermediate layer depends on the local concentration of the polymer. In our model, polymer is passively advected by the fluid and therefore, the viscosity profile of the middle-layer dynamically evolves with the velocity field in this region. The simplest non-trivial admissible solution of the underlying equations is the uniform motion of all three-layers having two planar interfaces separating these three layers. Stability of this system has been addressed earlier (Daripa and Pasa 1985a, 1986) for arbitrary viscosity profiles in the intermediate layer.

In this paper, our model allows diffusion of polymer in the above problem set-up. In a recent paper Daripa and Pasa (2007) first mathematically formulated this problem incorporating diffusion of polymer in the middle layer. In that paper, stability equations were derived in a form suitable for classical analysis which was then analyzed using weak formulation in order to obtain quantitative information about the effect of diffusion on flow instability. Such information were obtained in the form of upper bounds on the growth rate. The present paper develops a constructive method to obtain similar bounds as in Daripa and Pasa (2007) using numerical analysis. The method is constructive in the sense that the bounds are obtained by first developing a numerical scheme to solve the stability equations whose implementation and subsequent mining of numerical data to test the utility of the bound will be carried out in the future.

In most fluid flows, molecular diffusion slows down growth of instabilities except for some flows such as parallel shear flows. Such can not be said, without analytical justification, of the role of polymer diffusion in this problem since it’s role is somewhat different from that of molecular diffusion in fluid flows. In the middle layer, instabilities create non-uniformities in polymer concentration which in turn drives diffusion of polymer, an effect neglected thus far in the literature. This diffusion of polymer dynamically changes the local viscosity gradients in the middle-layer and the magnitudes

of jumps in viscosities across the interfaces which respectively drive the growth rates of instabilities in the middle-layer and on two interfaces. The extent to which growth of these instabilities is affected depends on the diffusion coefficient. Quantifying this effect in terms of diffusion coefficient can be useful in providing an insight into the overall effect of diffusion on the flow. In this paper, we investigate these issues using numerical discretization of the underlying stability equations.

In this paper, we obtain bounds on the growth rate using numerical analysis of the stability equations. The diffusion coefficient dependent bound obtained numerically clearly shows diffusive slowdown of instabilities which supports our results reported recently in Daripa and Pasa (2007). Since the method presented here relies on first developing a numerical scheme to solve the stability equations, the numerical scheme given here can be implemented, if so desired, to explore numerically the effects of diffusion on the modal growth rates and eigenfunctions of the normal modes. We must stress that these numerical implementation issues are not the subject of this paper, though we intend to undertake this task in the future.

It is important to emphasize here that the purpose of numerical analysis of the specific scheme carried out here is not so much as to just obtain a bound on a physical quantity (i.e. the maximal growth rate) but to ensure that the numerical scheme proposed for solving the stability equations has some desirable properties of the continuum equations that are useful to have before using the scheme for the purpose of numerical simulation. Numerically assessing the bound and assuring that it compares reasonably well with the exact bound which has been done in this paper precisely serves that purpose. This scheme then should be useful in computing the early stages of evolution of initial disturbances. The evolution of interfacial disturbances based on this scheme during initial stages then can be used as a benchmark for the purpose of validating any numerical calculation for the full initial value problem from which linear stability equations are derived. This is another motivation for the work carried out in this paper. Towards this end, it is also important to emphasize that the numerical analysis of the scheme presented here is non-trivial and not standard in the sense some ingenuity has been applied, in particular, in converting an invertible matrix to a invertible one (see section 4.1).

Since three-layer Hele-Shaw flows with diffusion, subject of this paper, partly builds upon two-layer Hele-Shaw flows, it is appropriate to add some relevant literature on various pertinent aspects of such two-layer flows which we do next in this paragraph. There have been extensive experimental, theoretical and numerical works on two-layer immiscible as well as miscible Hele-Shaw flows and the literature is so huge that we can barely cite only few of these. Earliest theoretical works on viscosity-jump driven interfacial instability of such two-layer immiscible flows date back to the late fifties works of Saffman and Taylor (1958), Saffman (1959) for Hele-Shaw flows and Chouke et.al. (1959) for flows in permeable media. Subsequently, there have been many studies on such two-layer flows such as exact non-trivial solutions in the form of fingers with or without surface tension (Escher and Simonnet 1996; Tian 1996; Kadanoff 1990, Vasconceles and Kadanoff 1991),

singularity formation (Nie and Tian 1998), numerical and perturbation studies (Almgren 1995; McLean and Saffman 1981), etc. For more exhaustive references on various numerical, experimental, and theoretical works, the review articles of Saffman (1986) and Kessler et.al. (1988) are worth mentioning. Towards this end, works of Hickernell and Yortsos (1986), Yortsos and Zeybek (1988); Loggia et. al. (1999), Shariati and Yortsos (2001) on two-layer miscible flows should also be cited.

In closing this section, we comment on how this work on Hele-Shaw flows relates to porous media. In porous media, transport of reactive as well as non-reactive species occur in myriad of processes either naturally and/or artificially by design, e.g., transport of contaminants, transport of biomass and solutes, transport of various species during various oil recovery processes, just to mention a few. In modeling such porous media flow processes involving a variety of species, diffusion of species naturally plays a significant role. Therefore, assessing the effect of species diffusion on various flow processes including hydrodynamic stability is important. This is what we do in this paper for immiscible flows using Hele-Shaw model as opposed to more appropriate Buckley-Leverett model, but this compromise has insignificant effect on the basic problem of diffusive slowdown we are addressing here. For example, displacement of oil by water in porous media by Buckley-Leverett model allows shock waves and rarefaction waves in saturation. Shock wave creates a jump in mobility across it whereas the saturation waves behind the shock wave creates a mobility gradient behind the shock. To a large extent, this is very well modeled using Hele-Shaw models instead with a sharp jump in viscosity (mobility) across the interface separating displaced and displacing fluids and a viscous profile behind the interface modeling the effect of rarefaction waves. The Hele-Shaw model that we consider below has all these properties.

## 2 Preliminaries

### 2.1 Problem Formulation

Fig. 1 shows a three-layer immiscible flow in a Hele-Shaw cell with two planar interfaces moving uniformly at a constant velocity. Our goal in this paper is to provide a constructive approach to study stability of this flow under proper setting that takes into account desired viscous profiles of these three layers and diffusion effects in the middle layer which are made precise below. As we will see, this study provides precise estimate of effect of diffusion on flow instabilities.

The flow in the Hele-Shaw cell is essentially two-dimensional:  $\Omega := (x, y) = \mathbb{R}^2$  with a periodic extension of the set-up in the  $y$ -direction. The uniform velocity far up-stream is  $\mathbf{u} = (U, 0)$  and the fluid in-between middle-layer of length  $L$  has a smooth viscous profile  $\mu(x)$  such that  $\mu_l < \mu(x) < \mu_r$ , where  $\mu_l$  and  $\mu_r$  are the viscosities of the fluids in the left and right extreme layers respectively (see Fig. 1). It is assumed that the middle-layer has an aqueous phase which is polymer-thickened-water (to be called 'poly-solution' henceforth) and the viscosity  $\mu$  of the poly-

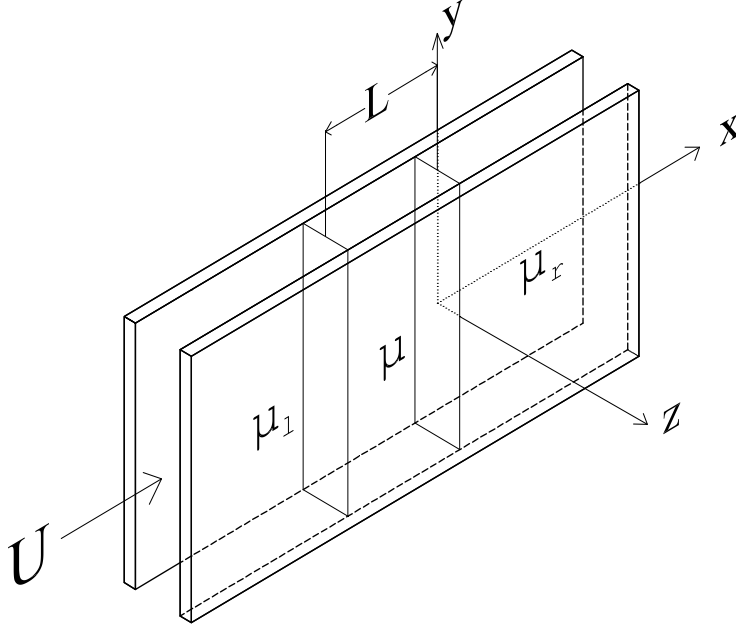


Figure 1: Three-layer fluid flow in a Hele-Shaw cell

solution is an invertible function of the polymer concentration  $c$ . Polymer concentration profile  $c(x)$ ,  $(-L < x < L)$  of the middle layer determines the viscous profile  $\mu(x)$  of this layer.

The case of passive advection of polymer by the fluid in the middle layer has been addressed earlier by several authors (Gorell and Homsy 1983; Daripa and Pasa 1985a). Thus, in this model, viscosity of every fluid element in the polysolution is a constant of motion. In this paper, we break this invariance property by also allowing diffusion of polymer in the middle layer which is more realistic. Hithertoo, this diffusion effect has not been addressed in this three-layer flow. The advection-diffusion equation of polymer in the middle layer is governed by

$$\frac{\partial c}{\partial t} + \mathbf{u} \cdot \nabla c = \eta \Delta c,$$

where  $\eta$ , the diffusion coefficient, is a constant. Since viscosity  $\mu$  is an invertible function of concentration  $c$ , the same equation holds true in the middle layer for viscosity  $\mu(x)$  in the middle layer. Therefore, the governing equations in each layer are

$$\nabla \cdot \mathbf{u} = 0, \tag{1}$$

$$\nabla p = -\mu \mathbf{u}, \tag{2}$$

$$\frac{\partial \mu}{\partial t} + \mathbf{u} \cdot \nabla \mu = \eta \Delta \mu, \tag{3}$$

where  $\nabla = \left( \frac{\partial}{\partial x}, \frac{\partial}{\partial y} \right)$  and  $\Delta$  is Laplacian in the plane. The first equation (1) is the continuity equation for incompressible flow, the second equation (2) is the Darcy's law (Darcy (1856))), and the third equation (3) is the advection-diffusion equation for viscosity.

The set-up shown in Fig. 1 and discussed at the beginning of this section is a basic solution of the above system with the following qualifications: the extreme layer viscosities  $\mu_l$  and  $\mu_r$  are constants and the viscous profile of the middle layer is linear, with viscosity increasing in the direction of flow in this layer. The pressure corresponding to this basic solution can be obtained by integrating (2). It is convenient to work in a moving frame with velocity  $(U, 0)$  so that the basic solution is stationary in this moving frame. Henceforth, our discussion including equations will be in the moving frame, unless otherwise mentioned. Here and below, with slight abuse of notation, the same variable  $x$  is used to refer to the  $x$ -coordinate in the moving reference frame.

## 2.2 Stability Equations

In the moving frame, the basic state is  $(u = 0, v = 0, p_0(x), \mu(x))$  where the basic viscous profile  $\mu(x)$  of the middle layer  $(-L < x < L)$  is linear, namely  $\mu(x) = a x + b$ , with viscosity increasing in the direction of flow from  $\mu(-L) > \mu_l$  to  $\mu(0) < \mu_r$  in this layer. If this basic state is perturbed by  $(\epsilon \tilde{u}, \epsilon \tilde{v}, \epsilon \tilde{p}, \epsilon \tilde{\mu})$ , where  $\epsilon$  is a small parameter, and the perturbed state  $(\epsilon \tilde{u}, \epsilon \tilde{v}, p_0(x) + \epsilon \tilde{p}, \mu(x) + \epsilon \tilde{\mu})$  is then substituted in the moving frame version of the equations (1) through (3), then we obtain the following linearized equations for  $\tilde{\mathbf{u}} = (\tilde{u}, \tilde{v})$ ,  $\tilde{p}$ , and  $\tilde{\mu}$  at the order  $O(\epsilon)$ .

$$\nabla \cdot \tilde{\mathbf{u}} = 0, \quad x, y \in \mathbb{R}, \quad (4)$$

$$\nabla \tilde{p} = -\mu \tilde{\mathbf{u}} - \tilde{\mu} (U, 0), \quad x, y \in \mathbb{R}, \quad (5)$$

$$\frac{\partial \tilde{\mu}}{\partial t} + \tilde{u} \frac{d\mu}{dx} = \eta \Delta \tilde{\mu}, \quad -L < x < 0. \quad (6)$$

Above equations are studied by the method of normal modes in which a typical wave disturbance has the form

$$(\tilde{u}, \tilde{v}, \tilde{p}, \tilde{\mu}) = (f(x), \psi(x), \phi(x), h(x)) e^{(i k y + \sigma t)}, \quad (7)$$

where  $k$  is a real axial wavenumber, and  $\sigma$  is the growth rate which could be complex. Substitution of (7) in (4) through (6) results in equations involving  $f(x)$ ,  $\psi(x)$ ,  $\phi(x)$ , and  $h(x)$  whose manipulation then leads to two coupled equations (see equations (8)<sub>1</sub> and (8)<sub>2</sub> below) involving  $f(x)$  and  $h(x)$ . These are subject to boundary conditions resulting from linearization of the kinematic and dynamic boundary conditions at two interfaces as derived in Daripa and Pasa (2006) for the zero-diffusion case. These boundary conditions are independent of diffusion process in the middle layer. Thus, in this model where the viscosity is advected as well as diffused by the fluid in the middle layer, the evolution of linearized disturbances is governed by the following problem.

$$\left. \begin{aligned} -(\mu f_x)_x + k^2 \mu f &= -k^2 U h, & x \in (-L, 0), \\ \eta h_{xx} - (\sigma + \eta k^2) h &= a f, & a > 0, \quad x \in (-L, 0), \\ f_x(0) &= (\lambda \mathcal{P} + q) f(0), & f_x(-L) = (\lambda r + s) f(-L), \\ h(0) &= h(-L) = 0, \end{aligned} \right\} \quad (8)$$

where  $\lambda = 1/\sigma$ ,  $a = (\mu(0) - \mu(-L))/L > 0$ ,  $\eta > 0$ , and  $\mathcal{P}$ ,  $q$ ,  $r$ ,  $s$  are defined by

$$\left. \begin{aligned} \mathcal{P} &= \{[\mu]_r U k^2 - T k^4\}/\mu(0), & q &= -\mu_r k/\mu(0) \leq 0, \\ r &= \{-[\mu]_l U k^2 + S k^4\}/\mu(-L), & s &= \mu_l k/\mu(-L) \geq 0. \end{aligned} \right\} \quad (9)$$

where  $[\mu]_r = (\mu_r - \mu(0))$  and  $[\mu]_l = (\mu(-L) - \mu_l)$ . It is worth noting that

$$\mathcal{P} \geq 0 \quad \text{for} \quad k^2 \leq k_1^2 = [\mu]_r U/T, \quad r \leq 0 \quad \text{for} \quad k^2 \leq k_2^2 = [\mu]_l U/S. \quad (10)$$

All these equations are in dimensional form. In (9),  $T$  is the surface tension at the interface  $x = 0$  and  $S$  is the surface tension at the interface  $x = -L$ . Note that the formulation here allows jumps in viscosities across the interfaces.

### 3 Numerical Approximation

The problem (8) is one-dimensional involving only independent variable  $x$ . We use a finite difference discretization of system (8) on  $(M - 1)$  equidistant interior points in the segment  $[-L, 0]$ :  $x_M = -L < x_{M-1} < x_{M-2} < \dots < x_1 < x_0 = 0$  and let  $d = (x_i - x_{i+1})$ . Then we have the unknowns  $f_0, f_1, f_2, \dots, f_M$  and  $h_1, h_2, \dots, h_{M-1}$  where  $f_i = f(x_i)$  and  $h_i = h(x_i)$ .

Using first-order approximation for derivatives at the end points in the boundary conditions (8)<sub>3</sub> and (8)<sub>4</sub>, we obtain

$$(f_0 - f_1)/d = (\mathcal{P}\lambda + q)f_0 \quad \Rightarrow \quad \left(\frac{1}{d\mathcal{P}} - \frac{q}{\mathcal{P}}\right)f_0 - \frac{1}{d\mathcal{P}}f_1 = \lambda f_0, \quad (11)$$

$$(f_{M-1} - f_M)/d = (r\lambda + s)f_M \quad \Rightarrow \quad \frac{1}{dr}f_{M-1} - \left(\frac{1}{dr} + \frac{s}{r}\right)f_M = \lambda f_M. \quad (12)$$

For interior points we use the central finite difference approximations to the derivatives such as

$$h_x(x) = \frac{h(x + d/2) - h(x - d/2)}{d}, \quad h_{xx}(x) = \frac{h(x + d) - 2h(x) + h(x - d)}{d^2}.$$

Using the above finite difference approximations, the discretized form of the system (8) becomes

$$A_{00}f_0 + A_{01}f_1 = \lambda f_0, \quad (13)$$

$$A_{ij}f_j = -k^2 U h_i, \quad \forall i \in [1, M - 1], \quad \forall j \in [0, M], \quad (14)$$

$$A_{M,M-1}f_{M-1} + A_{MM}f_M = \lambda f_M, \quad (15)$$

$$\{\eta B_{im} - (\sigma + k^2 \eta) \delta_{im}\} h_m = a f_i, \quad \forall i, m \in [1, M - 1]. \quad (16)$$

This system is overall first order accurate due to first order approximations (11) and (12) at the boundary. This makes the analysis and the results that we obtain below possible. In the above expressions,  $A_{ij}$  and  $B_{ij}$  are the conventional notations for the entries of the tridiagonal matrices

$\mathbf{A} \in \mathbb{R}^{(M+1) \times (M+1)}$  and  $\mathbf{B} \in \mathbb{R}^{(M-1) \times (M-1)}$  respectively which are given below. Above and below  $A_{i,i-1}$  means the entry  $A_{ij}$  when  $j = i - 1$ . Similarly for the entries of the matrix  $B$ .

$$A_{00} = \left( \frac{1}{d\mathcal{P}} - \frac{q}{\mathcal{P}} \right), \quad A_{01} = -\frac{1}{d\mathcal{P}}, \quad A_{0j} = 0, \quad \forall j \in [2, M]. \quad (17)$$

$$A_{i,i-1} = -\frac{\mu_{i-1/2}}{d^2}, \quad A_{ii} = \mu_i k^2 + \frac{\mu_{i-1/2} + \mu_{i+1/2}}{d^2}, \quad A_{i,i+1} = -\frac{\mu_{i+1/2}}{d^2}, \quad 1 \leq i \leq M-1 \quad (18)$$

$$A_{Mj} = 0, \quad \forall j < M-1; \quad A_{M,M-1} = \frac{1}{dr}, \quad A_{MM} = -\left( \frac{1}{dr} + \frac{s}{r} \right), \quad (19)$$

$$A_{ij} = B_{i,j} = 0 \quad \forall j \notin [i-1, i+1], \quad 1 \leq i \leq M-1, \quad (20)$$

$$B_{ii} = -\frac{2}{d^2}, \quad B_{i-1,i} = B_{i,i+1} = \frac{1}{d^2}, \quad 1 \leq i \leq M-1. \quad (21)$$

We obtain only one relation from (14) and (16) as follows. From (16) we have:

$$h_i = -\frac{a}{\sigma + k^2\eta} f_i + \frac{\eta}{\sigma + k^2\eta} B_{im} h_m, \quad \forall i \in [1, M-1]. \quad (22)$$

We use the above expression in (14) and get

$$A_{ij} f_j = -k^2 U h_i = (-k^2 U) \left\{ \frac{-a}{\sigma + k^2\eta} f_i + \frac{\eta}{\sigma + k^2\eta} B_{im} h_m \right\}, \quad \forall i \in [1, M-1], \quad (23)$$

where Einstein summation is implied for the subscripts  $m \in [1, M-1]$  and  $j \in [0, M]$ . We replace again  $h_m$ , by the expression (22) obtained from (14), in the last term of the right-hand side of the above formula (23). The final form of our discretized system (13)-(16) is given by the following set of equations.

$$A_{00} f_0 + A_{01} f_1 = \lambda f_0, \quad (24)$$

$$A_{ij} f_j = \frac{ak^2 U}{\sigma + k^2\eta} f_i + \frac{\eta}{\sigma + k^2\eta} B_{im} A_{mj} f_j, \quad (25)$$

$$A_{M,M-1} f_{M-1} + A_{MM} f_M = \lambda f_M, \quad (26)$$

where we recall that  $1 \leq i, m \leq (M-1)$  and  $0 \leq j \leq M$  for the system (25).

## 4 Approximate estimate of the growth rate

We let  $\sigma = \sigma_R + i\sigma_I$ , and  $\lambda = \lambda_R + i\lambda_I$ ,  $\sigma_R, \sigma_I, \lambda_R, \lambda_I \in \mathbf{R}$ . Below, we obtain estimate for the real part ( $\sigma_R$ ) of the growth rate. We consider (25) in the form (Einstein summation in (25) is replaced by conventional summation sign)

$$(\sigma + k^2\eta) \sum_{j=0}^M A_{ij} f_j = (ak^2 U) f_i + \eta \sum_{m=1}^{M-1} B_{im} \sum_{j=0}^M A_{mj} f_j; \quad i = 1, \dots, M-1. \quad (27)$$



We use the following notation (with the slight abuse of notation because  $y$  below has nothing to do with the  $y$ -coordinate of the set-up (see Fig. 1))

$$y_i = \sum_{j=0}^{j=M} A_{ij} f_j, \quad \text{for } i = 1, \dots, (M-1). \quad (28)$$

Therefore, the system (27) becomes

$$(\sigma + k^2 \eta) y_i = ak^2 U f_i + \eta \sum_{m=1}^{M-1} B_{im} y_m. \quad (29)$$

Let  $y^* = \max\{|y_i|, i = 1, 2, \dots, (M-1)\}$ . The following possibilities exist:

$$y^* = |y_1| \Rightarrow |\sigma + k^2 \eta - \eta B_{11}| \leq ak^2 U \frac{|f_1|}{|y_1|} + \eta |B_{12}|. \quad (30)$$

$$y^* = |y_j|, 1 < j < (M-1) \Rightarrow |\sigma + k^2 \eta - \eta B_{jj}| \leq ak^2 U \frac{|f_j|}{|y_j|} + \eta (|B_{j,j-1}| + |B_{j,j+1}|). \quad (31)$$

$$y^* = |y_n|, n = (M-1) \Rightarrow |\sigma + k^2 \eta - \eta B_{nn}| \leq ak^2 U \frac{|f_n|}{|y_n|} + \eta |B_{n,n-1}|. \quad (32)$$

We recall that  $k, B, \eta$  are real numbers, then we have the following inequality.

$$\sigma_R + k^2 \eta - \eta B_{mm} \leq |\sigma + k^2 \eta - \eta B_{mm}|.$$

In the relations (30), (31), and (32) we use the following relations.

$$\begin{aligned} B_{11} + |B_{12}| &= -2/d^2 + 1/d^2 \leq 0, \\ B_{jj} + |B_{j,j-1}| + |B_{j,j+1}| &= -2/d^2 + 1/d^2 + 1/d^2 = 0, \quad 1 < j < M-1, \\ B_{M-1,M-1} + |B_{M-1,M-2}| &= -2/d^2 + 1/d^2 \leq 0. \end{aligned}$$

From these inequalities and the relations (30)-(32) it follows that there exists an integer  $p$ ,  $1 \leq p \leq (M-1)$ , such that  $|y_p| = \max_j \{|y_j|, 1 \leq j \leq M-1\}$  (see (28)) for which

$$\sigma_R + k^2 \eta \leq ak^2 U \frac{|f_p|}{|y_p|}. \quad (33)$$

In the following, we obtain an estimate of the ratio  $|f_p|/|y_p|$ . For this, we first need to rewrite the system (14) in a suitable form because the matrix  $A_{ij}$ ,  $i = 1, \dots, (M-1)$ ;  $j = 0, 1, \dots, M$  of the system (14) is not a square matrix and hence not invertible. The following subsection discusses how to convert system (14) into a well-posed system. In particular, below we convert the non-square matrix associated with system (14) into a square matrix and then prove that this square matrix is invertible.

#### 4.1 A Well-posed System

In order to have only  $(M - 1)$  unknowns in the new system, we need to first express  $f_0$  in terms of  $f_1, f_2$  and express  $f_M$  in terms of  $f_{M-1}, f_{M-2}$ . For this, below we use the boundary condition  $(8)_5$  for  $h$  and the equation  $(8)_1$  to obtain a new form of the system (14) where only the unknowns  $f_1, f_2, \dots, f_{M-1}$  appear. Then we prove that the matrix of this new system is invertible.

The function  $h, f$  are smooth enough and we can consider that  $(8)_1$  holds also for  $x = 0$  and  $x = x_M$ . Then we have

$$-(\mu f_x)_x(x)|_{x=0} + k^2 \mu(0) f(0) = 0, \quad (34)$$

$$-(\mu f_x)_x(x)|_{x=x_M} + k^2 \mu(x_M) f(x_M) = 0. \quad (35)$$

We approximate the derivatives in (34) by a finite-difference formula:

$$(\mu f_x)_x(0) \approx \{(\mu f_x)(x_0) - (\mu f_x)(x_1)\}/d,$$

$$f_x(x_i) \approx \{f(x_i) - f(x_{i+1})\}/d,$$

then from (34) we obtain

$$f_0 = -\frac{\mu_0 + \mu_1}{\mu_0(k^2 d^2 - 1)} f_1 + \frac{\mu_1}{\mu_0(k^2 d^2 - 1)} f_2. \quad (36)$$

Similar expressions are used to approximate the derivatives in (35). Below we use the notation  $n = M - 1$  for ease of presentation and obtain

$$f_{n+1} = \frac{\mu_n + \mu_{n+1}}{\mu_{n+1}(1 - d^2 k^2)} f_n - \frac{\mu_n}{\mu_{n+1}(1 - d^2 k^2)} f_{n-1}. \quad (37)$$

We consider the first equation of the system (14) which after using (17) becomes

$$A_{10} f_0 + A_{11} f_1 + A_{12} f_2 = -k^2 U h_1.$$

Substituting (36) for  $f_0$  and the values of the coefficients  $A_{10}, A_{11}$  and  $A_{12}$  from (18) in the above equation, we obtain after some simplification

$$\left\{ \frac{-\mu_{1/2}}{d^2(1 - k^2 d^2)} \left( 1 + \frac{\mu_1}{\mu_0} \right) + \frac{\mu_{1/2} + \mu_{3/2}}{d^2} + k^2 \mu_1 \right\} f_1 + \left\{ \frac{\mu_{1/2} \mu_1}{d^2 \mu_0 (1 - k^2 d^2)} - \frac{\mu_{3/2}}{d^2} \right\} f_2 = -k^2 U h_1. \quad (38)$$

We consider also the last equation of the system (14)

$$A_{n,n-1} f_{n-1} + A_{n,n} f_n + A_{n,n+1} f_{n+1} = -k^2 U h_n, \quad n = M - 1.$$

We use (37), replace  $f_{n+1}$  in terms of  $f_n, f_{n-1}$  and obtain

$$\left\{ \frac{\mu_{n-1/2} + \mu_{n+1/2}}{d^2} + k^2 \mu_n - \frac{\mu_{n+1/2}}{d^2(1 - k^2 d^2)} \left(1 + \frac{\mu_n}{\mu_{n+1}}\right) \right\} f_n + \left\{ -\frac{\mu_{n-1/2}}{d^2} + \frac{\mu_n \mu_{n+1/2}}{d^2 \mu_{n+1}(1 - k^2 d^2)} \right\} f_{n-1} = -k^2 U h_n \quad (39)$$

If we let  $k d \ll 1$ , then

$$(1 - k^2 d^2) \approx 1. \quad (40)$$

Therefore in the formula (38)-(39) the denominators are not zero and the expressions (38) and (39) simplify to

$$\left\{ \frac{-\mu_{1/2}\mu_1 + \mu_0\mu_{3/2}}{d^2\mu_0} + k^2\mu_1 \right\} f_1 + \left\{ \frac{\mu_{1/2}\mu_1 - \mu_0\mu_{3/2}}{d^2\mu_0} \right\} f_2 = -k^2 U h_1, \quad (41)$$

and

$$\left\{ \frac{\mu_{n+1/2}\mu_n - \mu_{n+1}\mu_{n-1/2}}{d^2\mu_{n+1}} \right\} f_{n-1} + \left\{ \frac{\mu_{n+1}\mu_{n-1/2} - \mu_{n+1/2}\mu_n}{d^2\mu_{n+1}} + k^2\mu_n \right\} f_n = -k^2 U h_n. \quad (42)$$

Once the first and last equations of the system (14) are replaced by (41) and (42), the linear system (14) contains only the unknowns  $f_1, f_2, \dots, f_{M-1}$  and have a square matrix whose entries, now denoted by  $A'_{ij}$ ,  $i, j = 1, 2, \dots, (M-1)$ , are given by

$$A'_{11} = \frac{-\mu_{1/2}\mu_1 + \mu_0\mu_{3/2}}{d^2\mu_0} + k^2\mu_1, \quad A'_{12} = \frac{\mu_{1/2}\mu_1 - \mu_0\mu_{3/2}}{d^2\mu_0}, \quad A'_{1j} = A_{1j}, j = 3, \dots, (M-1). \quad (43)$$

$$A'_{ij} = A_{i,j}, \quad i = 2, \dots, (M-2); \quad j = 1, \dots, M-1 \quad (44)$$

$$\begin{aligned} A'_{nn} &= \frac{\mu_{n+1}\mu_{n-1/2} - \mu_{n+1/2}\mu_n}{d^2\mu_{n+1}} + k^2\mu_n, \quad n = M-1 \\ A'_{n,n-1} &= \frac{\mu_{n+1/2}\mu_n - \mu_{n+1}\mu_{n-1/2}}{d^2\mu_{n+1}}, \quad n = M-1 \\ A'_{M-1,j} &= A_{M-1,j}, \quad j = 1, \dots, (M-3). \end{aligned} \quad (45)$$

Note that the equations corresponding to  $i = 2, \dots, (M-2)$  of the initial system (14) remain the same.

It is easily verified that  $|A'_{ii}| > \sum_{j \neq i} |A'_{ij}|$  for each  $i \in [2, (M-2)]$ . If we have the same relation also for  $i = 1$  and  $i = (M-1)$ , then we can conclude that matrix  $\mathbf{A}'$  with entries  $A'_{ij}$ ,  $i, j = 1, 2, \dots, (M-1)$  is diagonally dominant and hence  $A'$  is an invertible matrix. Therefore we have to prove that  $|A'_{11}| > |A'_{12}|$  and  $|A'_{M-1,M-1}| > |A'_{M-1,M-2}|$  where elements of  $A'$  are defined in (43) and (45). That means we need to prove

$$\left| \frac{-\mu_{1/2}\mu_1 + \mu_0\mu_{3/2}}{d^2\mu_0} + k^2\mu_1 \right| > \left| \frac{\mu_{1/2}\mu_1 - \mu_0\mu_{3/2}}{d^2\mu_0} \right|. \quad (46)$$

$$\left| \frac{\mu_{n+1}\mu_{n-1/2} - \mu_{n+1/2}\mu_n}{d^2\mu_{n+1}} + k^2\mu_n \right| > \left| \frac{\mu_{n+1/2}\mu_n - \mu_{n+1}\mu_{n-1/2}}{d^2\mu_{n+1}} \right|. \quad (47)$$

Recall  $\mu(x) = ax + b$  which defines  $a = [\mu_0 - \mu(-L)]/L$ ,  $b = \mu_0$ . Hence

$$\mu_{1/2} = b - ad/2, \quad \mu_1 = b - ad, \quad \mu_{3/2} = b - 3ad/2,$$

$$\mu_n = ax_n + b, \quad \mu_{n+1} = ax_{n+1} + b, \quad \mu_{n-1/2} = ax_{n-1/2} + b, \quad \mu_{n+1/2} = ax_{n+1/2} + b.$$

Therefore

$$\frac{-\mu_{1/2}\mu_1 + \mu_0\mu_{3/2}}{d^2\mu_0} = -\frac{a^2}{2\mu_0},$$

and

$$\frac{\mu_{n+1}\mu_{n-1/2} - \mu_{n+1/2}\mu_n}{d^2\mu_{n+1}} = -\frac{a^2}{2\mu_{n+1}}.$$

We consider in (46) and (47) a large enough  $k$  and a small enough  $a$ , to have

$$k^2\mu_1 - \frac{a^2}{2\mu_0} > 0, \quad k^2\mu_n - \frac{a^2}{2\mu_{n+1}} > 0.$$

Consequently, the inequalities (46) and (47) are equivalent with

$$k^2\mu_1 > \frac{a^2}{\mu_0}, \quad k^2\mu_n > \frac{a^2}{\mu_{n+1}}. \quad (48)$$

The above inequalities hold for large enough  $l$  and  $k$ . Then we obtain  $|A'_{11}| > |A'_{12}|$ ,  $|A'_{M-1,M-1}| > |A'_{M-1,M-2}|$  and the matrix  $A'$  given by (43), (44) and (45) becomes invertible.

## 4.2 Diffusion Enhanced Stability Bounds on the Growth Rate

We will be using the inequality (33) to obtain a reasonable bound on the growth rate. For this, we first rewrite  $y_i$  defined in terms of entries of matrix  $A$  in (28) in terms of matrix  $A'$  which is

$$y_i = \sum_{m=1}^{m=M-1} A'_{im} f_m, \quad f_i = \sum_{j=1}^{j=M-1} \left( A'^{-1} \right)_{ij} y_j, \quad i = 1, \dots, (M-1) \quad (49)$$

where  $(A'^{-1})$  is the inverse of matrix  $A'$ . Using (49) in the inequality (33), it follows that

$$\sigma_R + k^2\eta \leq ak^2U \frac{|f_p|}{|y_p|} = ak^2U \frac{1}{|y_p|} \sum_{j=1}^{M-1} \left| \left( A'^{-1} \right)_{pj} y_j \right| \leq ak^2U \sum_{j=1}^{M-1} \left| \left( A'^{-1} \right)_{pj} \right| \frac{|y_j|}{|y_p|}.$$

We recall (see the line preceding (33))  $|y_p| = \max_j \{|y_j|, 1 \leq j \leq (M-1)\}$ . Using this in the above inequality for the estimate of the growth rate, we obtain the following estimate (50).

$$\sigma_R + k^2\eta \leq ak^2U \sum_{j=1}^{M-1} \left| \left( A'^{-1} \right)_{pj} \right|. \quad (50)$$

The matrix  $A'$  does not depend on  $\eta$ . Moreover we have  $A'^{-1} \approx O(d^2)$  and  $A'^{-1} \approx O(1/k^2)$  because  $A' \approx O(1/d^2)$  and  $A' \approx O(k^2)$ . Then from (50) we obtain the following conclusion: real part of the growth rate is negative with diffusion.

In the case of very small wavenumbers  $k$ , we use the system (25) with  $k^2 \approx 0$ . Therefore, we obtain from (27)

$$(\sigma/\eta) \sum_{j=0}^{j=M} A_{ij} f_j = \sum_{m=1}^{M-1} B_{im} \sum_{j=0}^M A_{mj} f_j, \quad i = 1, \dots, (M-1)$$

and  $(\sigma/\eta)$  is an eigenvalue of the matrix  $B_{im}$ , with eigenvectors  $\sum_{j=0}^{j=M} A_{mj} f_j$ . In this case, we do not need a new system, and the initial matrix  $A_{ij}$  does not depend on  $k$  and  $\eta$ . Recall the definition (21) of the matrix  $B$ . The sum of the elements of each line of  $B$  is negative and hence we obtain  $\sigma/\eta \leq 0$ . This shows diffusive (diffusion of polymer) slowdown of instabilities.

## 5 Comparison between Exact and Approximate Estimates

An estimate of the upper bound similar to the one given above by (33) can be derived from the results we have obtained in Daripa and Pasa (2007) using exact (weak formulation) analyses of the exact system (8). To see this, recall the following estimates we obtained in Daripa and Pasa (2007).

$$\sigma_R \leq \frac{aF_1}{\int_{-L}^0 |h|^2 dx} - k^2 \eta \leq \frac{a|F_1|}{\int_{-L}^0 |h|^2 dx} - k^2 \eta,$$

where  $\sigma_R = \text{real}(\sigma)$  and  $F_1$  is the real part of the inner product  $\int_{-L}^0 f(-h)^* dx$  (see Daripa and Pasa (2007)). Since

$$|F_1| \leq \sqrt{\left(\int_{-L}^0 |f|^2 dx\right) \left(\int_{-L}^0 |h|^2 dx\right)},$$

which follows from Cauchy-Schwartz-Buniakowsky inequality, we get

$$\sigma_R \leq a \sqrt{\frac{\int_{-L}^0 |f|^2 dx}{\int_{-L}^0 |h|^2 dx}} - k^2 \eta. \quad (51)$$

We use the rectangle rule to approximate the two integrals appearing in (51). We have

$$\begin{aligned} \int_{-L}^0 |f|^2 dx &\approx |f_1|^2 d + |f_2|^2 d + |f_3|^2 d + \dots + |f_{M-1}|^2 d, \\ \int_{-L}^0 |h|^2 dx &\approx |h_1|^2 d + |h_2|^2 d + |h_3|^2 d + \dots + |h_{M-1}|^2 d, \end{aligned}$$

where  $d$  is the discretization step used in section 3. Therefore we get

$$\frac{\int_{-L}^0 |f|^2 dx}{\int_{-L}^0 |h|^2 dx} \approx \frac{|f_1|^2 d + |f_2|^2 d + |f_3|^2 d + \dots + |f_{M-1}|^2 d}{|h_1|^2 d + |h_2|^2 d + |h_3|^2 d + \dots + |h_{M-1}|^2 d} \leq \max_i \left\{ \frac{|f_i|^2}{|h_i|^2} \right\}, \quad 1 \leq i \leq M-1.$$

From the relations (28) and (14) we have  $h_i = -y_i/k^2U$ . Therefore, from the above formula, it follows that

$$\sigma_R \leq ak^2U \max_i \frac{|f_i|}{|y_i|} - k^2\eta. \quad (52)$$

This bound obtained from numerical approximation of the exact formulae of the upper bound (Daripa and Pasa 2007) is also implied by (33) which is seen as follows. Since  $|y_p| = \max_j |y_j|$  in (33) (see the line before inequality (33)), it follows that

$$\frac{|f_p|}{|y_p|} \leq \max_i \frac{|f_i|}{|y_i|}$$

and hence inequality (33) can also be written as

$$\sigma_R \leq ak^2U \max_i \frac{|f_i|}{|y_i|} - k^2\eta. \quad (53)$$

Thus we see from (52) and (53) that both procedures give the same formula and in this sense, the presented numerical method of this paper is convergent.

We want to emphasize that in Daripa and Pasa (2007) using a variational formulation, we obtained an exact formula for the upper bound from which we show how to obtain the above estimate (52) which is same as (53) obtained in this paper using numerical analysis. Thus both methods, whether exact or approximate (see (52) and (53)), lead to the same estimate. However, since this estimate is not exclusively in terms of the data of the problem but rather depends also on the eigenfunction  $f$ , this formula is not very useful for computing exact numerical values of modal upper bounds. In contrast, in addition to the estimate (33) or equivalently (53), we obtain *another explicit estimate* (50) *which is in terms of data of the problem*. The unknown ratio  $|f_i|/|y_i|$  does not appear any more in this formula (50). From this, we also see that a large value of diffusion coefficient has the potential to completely stabilize the flow, a conclusion also reached in Daripa and Pasa (2007).

Exact computation of the upper bound either from (52) or (53) is not possible in the context of this paper since the estimate (52) depends on eigenfunction  $f$  which is not known until the differential equations modeling this problem are solved computationally which falls outside the scope of this work. Present work, as stated early in the abstract, is about the establishment of stabilizing role of diffusion on hydrodynamic instability using a constructive approach which has been accomplished in this paper. The bound (52) or (53) on growth rate is for individual waves due to dependency of the estimate on the wavenumber  $k$ . We can compute the values of modal upper bound for individual waves from (52) or (53) (which is implied by (33)) provided we assume, for the purpose exposition of the effect of diffusion on stability which is the main purpose of this paper set at the outset, the value of  $\min_i |f_i|/|y_i|$ , minimum taken over all  $i$ . We plot modal upper bound against the wavenumber  $k$  taking  $\min_i |f_i|/|y_i| = 10/(aU)$  and  $\eta = 4$  (recall that  $a$  is the slope of the basic profile of the viscosity and  $\eta$  is the viscosity coefficient). There is no specific reason

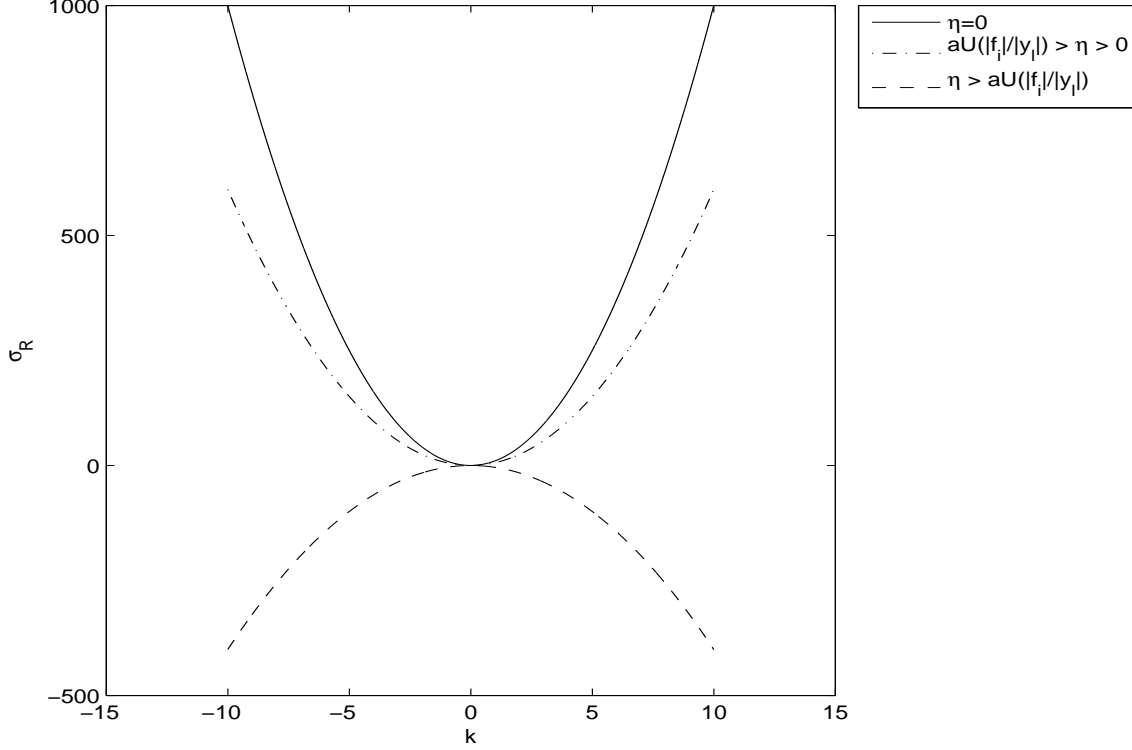


Figure 2: Stabilizing effect of diffusion: plots of modal upper bound on the growth rate versus wavenumber with and without diffusion. The solid curve is for case with no diffusion and other curves for cases with diffusion.

behind these numbers. Any other choice will do as well to reveal the qualitative nature of the plots in Fig. 2. Figure 2 shows plots of the upper bound for individual waves against the wavenumber for three cases: (i) solid curve is for the case with no diffusion; (ii) dash-and-dotted curve is for the case with diffusion for modest values of diffusion coefficient  $\eta$  (specifically when  $aU \frac{|f_i|}{|y_l|} > \eta$ ); (iii) dashed curve is also for the case with diffusion but for very large values of diffusion coefficient (specifically when  $aU \frac{|f_i|}{|y_l|} < \eta$ ). These figures show the stabilizing effect of diffusion and in extreme situation (the dashed curve), the flow can be completely stabilized.

## 6 Conclusion

The constructive approach of this paper (see section 4) and the weak formulation approach of Daripa and Pasa (2007) provide similar estimates (33) and (52) respectively for the real part of the growth rate. Moreover, the formula (50) in this paper and the Theorem 1 in Daripa and Pasa (2007) clearly show that species diffusion suppresses instability. For appropriate values of the parameters of our model, a large enough diffusion coefficient can reverse the instability process. As a function of the wavenumbers, the growth rate is bounded by a parabola with a maximum point (with the

leading term  $-\eta$ ) given by the estimate (50).

The result in the paper was obtained for a deeper reason using the specific the numerical scheme since the bound on a physical quantity obtained numerically can depend on the specific numerical scheme. To some extent, devising the numerical scheme (see section 3) for solving the non-standard eigenvalue problem (8) (see section 2.2) is analogous to devising an appropriate numerical scheme (with a proper choice of numerical parameters) for solving the full time-dependent initial value problem (see the problem posed by (1), (2) and (3)) so that numerical dispersion well approximates the exact dispersion relation. In numerically solving the initial value problem of the time dependent system set in section 2.1 subject to any initial data close to the basic state, the initial stage of evolution needs to be compared (and thus have confidence in the simulation results) against the solution predicted by the linear stability problem (8) of section 2.2, which basically amounts to computing the spectrum of (8) as accurately as possible. That means one must have a scheme to compute the spectrum that faithfully represents the actual spectrum of (8). The only known theoretical result of this problem (8) is the upper bound reported in Daripa and Pasa (2007). Since the proposed numerical scheme in this paper has comparable bounds, the proposed scheme is a suitable candidate for implementation and subsequently using the numerical results for short time as a benchmark for the full initial value problem (see section 2.1).

Finally, it is worth mentioning in what respects immiscible flows in a Hele-Shaw cell considered here is different from similar flows in porous media and also from miscible flows either in porous media or in a Hele-Shaw cell. Since immiscible phases in a Hele-Shaw cell are treated distinct with distinct sharp boundaries separating these phases, field equations (1)-(3) do not involve surface tension. Surface tension rather appears in the boundary conditions (8)-(9) which arise from the balance of forces at the interfaces. The derivation of these equations is standard and has been addressed in Daripa and Pasa (2004, 2006). In contrast, such immiscible flows in porous media models mixing between phases at microscopic level using Buckley-Leverett equation and allows inclusion of capillary pressure, which is related to the surface tension and the Leverett function, directly into the field equations (rather than in the interfacial boundary conditions).

## 7 Acknowledgments.

The second author thanks the Department of Mathematics at Texas A&M University for hospitality during a summer visit. Support from CERES (2004) program is also acknowledged here. We also thank two anonymous referees and the editor, Jacob Bear, for their constructive criticisms.



## References

- [1] Almgren, R.F.: Crystalline Saffman and Taylor fingers. *SIAM J. Appl. Math.* **55**, 1511-1535 (1995)
- [2] Chouke, R.L., van Meurs, P., van der Poel, C.: The stability of a slow, immiscible, viscous liquid-liquid displacements in a permeable media. *Petrol. Trans. AIME* **216**, 188-194 (1959)
- [3] Daripa, P., Glimm, J., Lindquist, B. McBryan, O.: Polymer Floods: A Case Study of Nonlinear Wave Analysis and Instability Control in Tertiary Oil Recovery. *SIAM J. Appl. Math.* **49** 353-373 (1988)
- [4] Daripa, P., Pasa, G.: An Optimal Viscosity Profile in Enhanced Oil Recovery by Polymer Flooding. *Int. J. Engg. Sci.* **42** 2029-2039 (2004)
- [5] Daripa, P., Pasa, G.: New bounds for stabilizing Hele-Shaw flows. *Appl. Math. Lett.* **18(11)**, 1293-1303 (2005a)
- [6] Daripa, P., Pasa, G.: On the Growth Rate for Three-Layer Hele-Shaw Flows: Variable and Constant Viscosity Cases. *Int. J. Engg. Sci.* **43(11-12)** 877-884 (2005b)
- [7] Daripa, P., Pasa, G.: A simple derivation of an upper bound in the presence of viscosity gradient in three-layer Hele-Shaw flows. *J. Stat. Mech.* 11 pages, P01014 (2006) doi:10.1088/1742-5468/2006/01/P01014
- [8] Daripa, P., Pasa, G.: Stabilizing Effect of Diffusion in Enhanced Oil Recovery and Three-Layer Hele-Shaw Flows with Viscosity Gradient. *Transp. Porous. Media.* **70(1)** 11-23 (2007)
- [9] Escher, J., Simonett, G.: On Hele-Shaw models with surface tension, *Math. Res. Lett.* **3**, 467-474 (1996)
- [10] Hickernell, F.J., Yortsos, Y.C.: Linear stability of miscible displacement processes in porous media in the absence of dispersion *Stud. Appl. Math.* **74**, 93-115 (1986)
- [11] Gorell, S.B., Homsy, G.M.: A theory of the optimal policy of oil recovery by the secondary displacement process. *SIAM J. Appl. Math.* **43**, 79-98 (1983)
- [12] Kadanoff, L.P.: Exact Solutions for the Saffman-Taylor Problem with Surface Tension. *Phys. Rev. Letts.* **65**, 2986-2988 (1990)
- [13] Kessler, D.A., Koplik, J., Levine, H.: Pattern selection in fingered growth phenomena. *Adv. in Phys.* **37**, 255-329 (1988)

- [14] Littman, W.: *Polymer Flooding: Developments in Petroleum Science*. **24** Elsevier, Amsterdam (1988)
- [15] Loggia, D., Rakotomalala, N., Salin, D., Yortsos, Y.C.: The effect of mobility gradients on viscous instabilities in miscible flows in porous media. *Phys. Fluids*. **11(3)**, 740-742 (1999)
- [16] McLean, J.W., Saffman, P.G.: The effect of surface tension on the shape of fingers in a Hele-Shaw cell. *J. Fluid Mech.* **102**, 445-469 (1981)
- [17] Needham, R.B., Doe, P. H.: Polymer flooding review. *J. Pet. Technol.* **12**, 1503-1507 (1987)
- [18] Nie, Q., Tian, F.R.: Singularities in Hele-Shaw flows. *SIAM J. Appl. Math.* **58**, 34-54 (1998)
- [19] Saffman, P.G.: Exact solutions for the growth of fingers from a flat interface between two fluids in a porous medium or Hele-Shaw cell. *Quart. J. Mech. Appl. Math.* **12**, 146-155 (1959)
- [20] Saffman, P.G.: Viscous Fingering in Hele-Shaw Cells. *J. Fluid Mech.* **173**, 73-94 (1986)
- [21] Saffman, P.G., Taylor, G.I.: The penetration of a fluid in a porous medium or Hele-Shaw cell containing a more viscous fluid. *Proc. Roy. Soc. A.* **245**, 312-329 (1958)
- [22] Shah, D., Schechter, R.: *Improved Oil Recovery by Surfactants and Polymer Flooding*, Academic Press, New York (1977)
- [23] Shariati, M., Yortsos, Y.C.: Stability of miscible displacements across stratified porous media. *Phys. Fluids*. **13(8)**, 2245-2257 (2001)
- [24] Sorbie, K.S.: *Polymer-Improved Oil Recovery*. CRC Press, Boca Raton, Florida (1991)
- [25] Tian, F.R.: A Cauchy integral approach to Hele-Shaw problems with a free boundary: the case of zero surface tension, *Arch. Ration. Mech. Anal.* **135**, 175-196 (1996)
- [26] Uzoigwe, A.C., Scanlon, F.C., Jewett, R.L.: Improvement in polymer flooding: The programmed slug and the polymer-conserving agent. *J. Petrol. Tech.* **26**, 33-41 (1974)
- [27] Vasconceles, G.L., Kadanoff, L.P.: Stationary solutions for the Saffman-Taylor problem with surface tension. *Phys. Rev. A.* **44**, 6490-6495 (1991)
- [28] Yortsos, Y.C., Zeybek, M.: Dispersion driven instability in miscible displacement in porous-media. *Phys. Fluids*. **31(12)**, 3511-3518 (1988)